

# Causal and homogeneous networks

P. Białas , Z. Burda and B. Wacław

*M.Smoluchowski Institute of Physics, Jagellonian University, Reymonta 4, 30-059 Krakow, Poland*

**Abstract.** Growing networks have a causal structure. We show that the causality strongly influences the scaling and geometrical properties of the network. In particular the average distance between nodes is smaller for causal networks than for corresponding homogeneous networks. We explain the origin of this effect and illustrate it using as an example a solvable model of random trees. We also discuss the issue of stability of the scale-free node degree distribution. We show that a surplus of links may lead to the emergence of a singular node with the degree proportional to the total number of links. This effect is closely related to the backgammon condensation known from the balls-in-boxes model.

## INTRODUCTION

Many real-world complex networks have heavy tails in the node degree distribution [1, 2, 3]. It was a great discovery [4] to realize that networks with such a property can be naturally produced by a preferential attachment growth [5]. It has become an important issue to work out the consequences of the presence of heavy tails in the degree distribution on topological properties of networks [1, 2, 3].

The degree distribution however gives only a crude information about topology of random networks unless it is supplemented by some other information. Let us take as an example  $k$ -regular graphs. They are defined as graphs with all nodes having degree equal  $k$ . The node degree distribution of  $k$ -regular graphs is  $p(q) = \delta_{qk}$  independently of the graph topology. A regular equilateral triangulation or a cubic lattice are perfect examples of 6-regular graphs but they have completely different topological and geometrical properties: the triangulation has fractal dimension two while the cubic lattice – three. One can see the difference when one determines for example the number of nodes in the given distance from the given node.

The two examples of 6-regular graphs are not random graphs so one could argue that maybe if one considered random graphs from the ensemble of 6-regular graphs one would see statistically identical topological and geometrical properties of them. But to answer this question one has to define what a random graph is. One can do it by introducing a statistical ensemble of graphs [6, 7, 8, 9, 10, 11, 12, 13, 14]. This means that one has to specify the set of graphs which one wants to study: as for instance  $k$ -regular graphs, trees, simple graphs, pseudographs, etc., their attributes: directed, undirected, Eulerian, connected, etc. Then one has to define a probability measure on this set by ascribing to each graph from the set a positive number. This number gives (after normalization) the probability that the graph will be selected when the set is sampled randomly. The statistical properties of the ensemble heavily depend on the choice of the

probability measure.

The classical example of this approach is the ensemble of Erdős-Rényi graphs [15, 16, 17]. The set of graphs consists of all graphs with  $N$  nodes and  $L$  links having neither multiple- nor self-connections. The measure in the Erdős-Rényi ensemble is defined as follows [14]. One labels all nodes by the integers  $1; \dots; N$  to obtain labeled graphs. Such graphs are isomorphic to  $N \times N$  symmetric adjacency matrices with  $L$  entries equal to one in the upper triangle (and symmetrically also in the lower triangle). Each labeled graph (adjacency matrix) has the same statistical weight. The partition function reads:

$$Z_h = \sum_{lg} 1 = \sum_g n_h(g); \quad (1)$$

The index  $h$  stands for homogeneous and will be explained later. The first sum runs over all labeled graphs, the second over graphs (=unlabeled graphs). By a graph we mean graph's topology that is the shape or skeleton which one obtains when one removes the labels. The number  $n_h(g)$  of distinct labelings (adjacency matrices) of the graph  $g$  depends on  $g$  and thus some graphs are more whereas some are less probable in this ensemble.

One should realize that the definition (1) assumes that a) we can distinguish the vertices of the graph, b) we are only interested in properties that do not depend on the labelings. The permutation of indices neither changes graphs topology nor physical quantities measured on this graph. The model has thus permutation symmetry and one should divide out the volume of the permutation group. One could explicitly write the factor of  $1=N!$  instead of 1 in the sum (1). However, as long as  $N$  is fixed this factor is constant and therefore can be pulled out in front of the sum and skipped as an irrelevant normalization of the partition function. One should keep it in any formula for an ensemble with varying  $N$  as we will do in the next section (see for example (4)). The origin of this factor is the same as in classical statistical mechanics for identical particles. These assumptions are reasonable for many real-world examples of graphs, but one must be aware that they can be violated. For example when considering chemical compounds we must treat the vertices of the same kind as indistinguishable similarly as in quantum statistics. Then we should use an ensemble where each graph topology has the same weight:  $Z = \sum_g 1$ . In practice such a definition turns out to be much more difficult to handle [18]. Also the ensembles, where the probability of selecting a given graph depends on its labels, appear naturally when one considers ensembles of growing networks [25, 27].

In the Erdős-Rényi ensemble (1) all labeled graphs are equiprobable. One can however weight the graphs in a way which depends on their topology: for example one can introduce correlations between neighboring nodes degrees [8, 21], one can favor loops [10] which are very rare for the Erdős-Rényi graphs, or one can introduce a weight which modifies the node-degree distribution [6, 28]. In the last example one does it by modifying the partition function to the following form:

$$Z_h = \sum_{lg} w(q_1)w(q_2) \dots w(q_N); \quad (2)$$

where  $q_k$  is the degree of  $k$ -th node and  $w(q)$  is an arbitrary weight function. One can tune the weight function  $w(q)$  in order to obtain graphs with a desired probability distribution.

In this way one can produce for example scale-free graphs with the Barabási-Albert degree distribution [6, 14].

In this contribution we apply the concepts of statistical mechanics like statistical ensembles, partition function, averages over ensemble, and so forth to study random graphs. Within this approach one has already obtained many interesting results [6, 7, 8, 9, 10, 11, 12, 13, 14]. This approach is a straightforward generalization of the Erdős-Rényi ideas.

At the first glance one can think that the statistical mechanics is not adequate for growing networks which are not in equilibrium. Indeed such ensembles cannot be understood as equilibrium ensembles with the Gibbs measure, having temperature etc. One should rather understand them as follows. Imagine that one repeats the process of growth many times independently and each time one terminates it when the network reaches a given size. One obtains a collection of networks which occur with a certain probability. This perfectly defines an ensemble of graphs [7, 25]. It is not an equilibrium ensemble but all methods of statistical mechanics work, so one can use them. In order to distinguish growing networks which are inhomogeneous from homogeneous graphs discussed above (for which all nodes are treated equally as for instance for Erdős-Rényi graphs) we shall call the growing networks - *causal*, and the networks obtained from arbitrarily labeled graphs - *homogeneous*. The difference will become clear in the next section. Anticipating some results, the causal and homogeneous networks have different geometrical features even if they have identical node-degree distributions.

## CAUSAL VERSUS HOMOGENEOUS NETWORKS

Vertices of a growing network can be labeled by integers representing the order of attachment to the network. It is clear that not all possible labelings of the underlying graph can be realized in this way (see figure 1). We will call those that can be – *causal* labelings or equivalently we will say that the labels are causally ordered. A necessary condition for a causal labelings is that a) root has the smallest label and b) one can connect every vertex to the root<sup>1</sup> by a path (not necessarily the shortest) in such a way that the labels on it are increasing from the root. It implies a condition that every vertex except the root must have at least one neighbor with a smaller label.

As in the previous section we can define a partition function for the ensemble of equiprobable rooted graphs with causal ordering:

$$Z_{cNL} = \sum_{clg} 1 = \sum_g n_c(g): \quad (3)$$

The first sum is done over all causally labeled graphs  $clg$ . This ensemble is a counterpart of the Erdős-Rényi ensemble (4) for homogeneous graphs in the sense that all labeled graphs are equiprobable. The difference between the two is that only causal labelings are allowed here. The second sum in (3) is done over all graphs  $g$ . Each graph is weighted in

---

<sup>1</sup> Obviously we are considering only connected graphs. For disconnected graph this condition must be suitably modified.

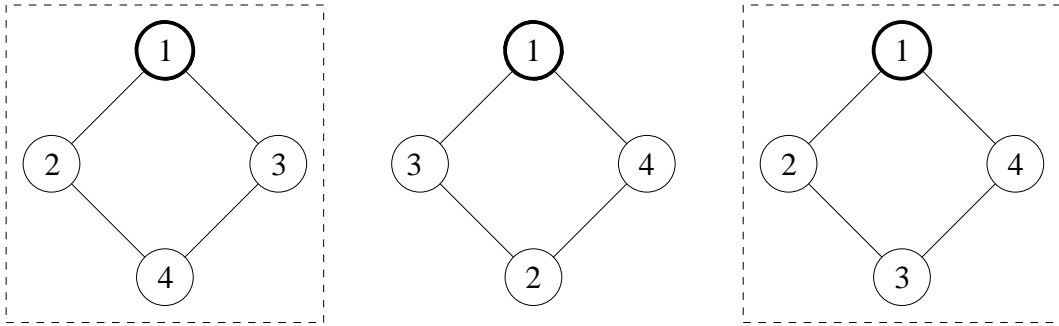


**FIGURE 1.** Examples of labelings of a simple graph. Two labelings marked with the dashed rectangle are causal. The labeling in the middle is not. Also the remaining nine labelings of this graph (not shown on the picture) are not causal because the root does not have the label one.

the sum by the number of its causal labelings. This number is smaller than the number of all labelings  $n_h(g)$  of this graph. Although the partition functions (1) and (3) cover the same set of graph topologies  $fgg$ , their statistical weights are different. When one samples graphs randomly in the homogeneous graphs ensemble (1) one thus observes different probabilities of graphs' (topologies') occurrence than in the ensemble of causal graphs.

This can be illustrated by calculating various quantities for random tree graphs (branched polymers) for which the calculations can be done analytically [19, 20, 21, 22, 23, 24, 25, 26, 27].

Let us give a short account on results of those calculations. We shall discuss ensembles of planted rooted trees. Each graph in such an ensemble is connected and has no loops. One node of the graph has a single line sticking from it interpreted as the stem of the tree (we omit the root node at the end of the stem). The number of branches (links)  $L$  of a tree with  $N$  nodes is equal to  $N - 1$ . The stem is not counted as a branch. Because  $L$  is related to  $N$  we can skip  $L$  in the  $Z_{hNL}$  and denote the canonical partition function for trees by  $Z_{hN}$ . The grand canonical partition function for homogeneous planted trees is

$$Z_h(x) = \sum_{N=1}^{\infty} \frac{Z_{hN}}{N!} x^N \quad (4)$$

and can be represented as a bubble in figure 2. The free end of the bubble denotes the stem while the bubble – the sum over all trees weighted as in (4). One can write an identical definition for causal trees. For technical reasons instead of the chemical potential  $\mu$  in the grand-canonical partition function (4) we prefer to use the fugacity  $x = e^{\mu}$ .

An advantage of using the grand-canonical partition function is that one can deduce a closed formula [25] expressing  $Z_h(x)$  as a function of itself:

$$Z_h(x) = x \sum_{k=0}^{\infty} \frac{1}{k!} Z_h^k(x) = x e^{Z_h(x)}; \quad (5)$$

which can be graphically represented as in figure 2. The meaning of this graphical equation is the following. Any rooted tree can be constructed by joining stems of a

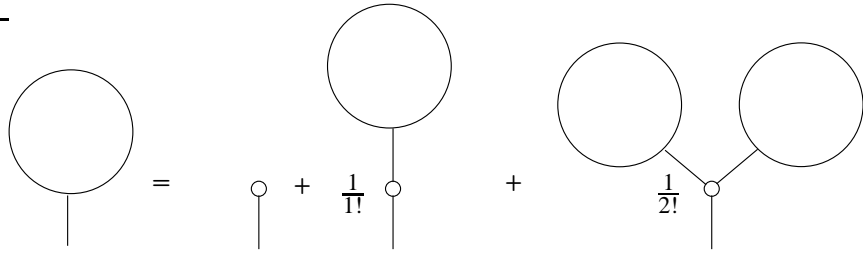


**FIGURE 2.** Graphical representation of the self-consistency equation (5). The bubble contains the grand-canonical sum over planted rooted trees. Each tree is weighed with the size factor  $x^N$  and the small circle representing a single node gives additional factor  $x$ .

certain number of trees at a common node and attaching a new common stem to this node. If one sums over all trees in each bubble on the right-hand side of the graphical equation shown in figure 2, one obtains a sum over all trees also on the left-hand side. In order to obtain the partition function  $Z_h(x)$  (4) one has to take care of the power of  $x$  which counts the number of vertices. We see that the new tree has by one vertex more than all subtrees used in the construction so one has to multiply the right-hand side by  $x$ . In order to avoid overcounting while joining  $k$  trees, which now form  $k$  branches of the new tree, one has to divide out the factor  $k!$  which counts the number of indistinguishable ways in which one can put the trees together. Thus the expression  $Z_h^k$  which represents the composition of  $k$  subtrees is divided by  $k!$ . Finally, one has to sum over  $k$  to include all branching possibilities at the root. In this way one reproduces the partition function  $Z_h$  on the left-hand side and  $x \exp(Z_h)$  on the right-hand side of eq. (5).

Using the equation (5) one can determine  $Z_{hN}$  by inverse Laplace transform (here written as a contour integral):

$$Z_{hN} = \frac{N!}{2\pi i} \int^{\Gamma} \frac{dx}{x^{N+1}} Z_h(x) : \quad (6)$$

Changing the integration variable from  $x$  to  $Z = Z_h(x)$  and by means of (5) one obtains

$$Z_{hN} = \frac{N!}{2\pi i} \int^{\Gamma} \frac{dZ}{Z^N} e^{NZ} (1 - Z) = N! \left( \frac{N^{N-1}}{(N-1)!} - \frac{N^{N-2}}{(N-2)!} \right) = N^{N-1} : \quad (7)$$

This result tells us that there are  $N^{N-1}$  labeled planted rooted trees of size  $N$ . There is one planted rooted tree for  $N = 1$ , two for  $N = 2$ , nine for  $N = 3$ , etc. The labeled trees for  $N = 1, 2, 3$  are shown in figure 3. Note that if one removes the stem one obtains an ensemble with one marked vertex - the tree is not planted anymore. The number of trees with one marked vertex is thus also equal to  $N^{N-1}$ . From this one can deduce the number of all labeled trees without any marked vertex. On a tree with  $N$  vertices one can mark one of  $N$  vertices, so the number of trees with a marked vertex must be  $N$  times larger than the total number of labeled trees. Thus the number of labeled trees of size  $N$  is  $N^{N-2}$ . This is the classical result derived first by Cayley (see reference [32] for general introduction on counting graphs).

Let us come back to planted rooted trees, but now consider only causally labeled ones. For the trees we have exactly one path joining any given vertex and the root and along

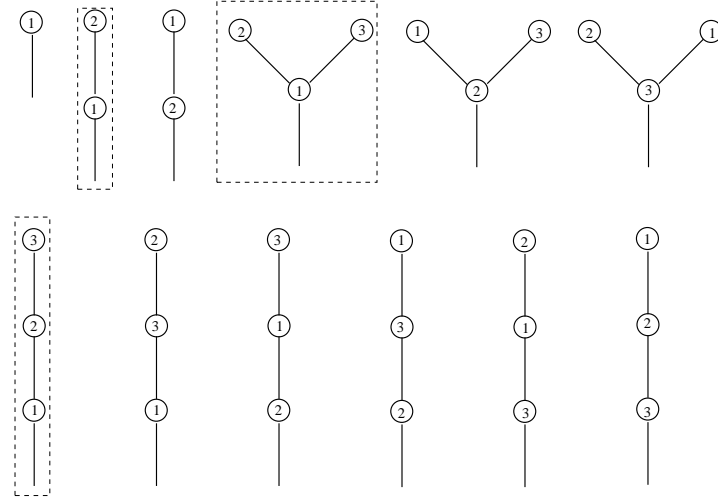


**FIGURE 3.** Planted rooted trees of size  $N = 1; 2; 3$ . Causal labelings are marked with dashed rectangles.

this path labels must increase from the root outwards (see figure 3). One can derive [25] a self-consistency equation for causal planted rooted trees similarly to (5). It has the same logical structure as the graphical equation shown in figure 2 but the causality imposes a requirement on labels ordering. A careful analysis of the consequences implied by this requirement shows that one obtains the following self-consistency equation for causal trees [25]:

$$\frac{dZ_c(x)}{dx} = e^{Z_c(x)}: \quad (8)$$

This equation can be solved for  $Z_c$  yielding:

$$Z_c(x) = -\ln(1-x) = \sum_{N=1}^{\infty} \frac{1}{N} x^N = \sum_{N=1}^{\infty} \frac{Z_{cN}}{N!} x^N; \quad (9)$$

and hence:

$$Z_{cN} = (N-1)!: \quad (10)$$

Thus there are  $(N-1)!$  causally labeled planted rooted trees. For example, there is one for  $N=1$ , one for  $N=2$  and two for  $N=3$ , etc. One can easily find these trees among all labeled trees in figure 3. Causally labeled trees form a small subset of all labeled trees: the fraction of causally labeled trees  $Z_{cN} = Z_{hN} N^{3/2} e^{-N}$  quickly disappears when the size of the system grows. One may ask whether the statistical properties of this subset are identical as of the whole set. The answer is that they are completely different. Probably the most striking difference is that the causal trees are much more compact and have much smaller linear extent than homogeneous trees.

One can quantify this statement by checking how the average distance between nodes depends on the size of the tree. One defines geodesic distance  $r_{ab}$  for each pair of vertices  $a, b$  as the number of links of the (shortest) path between  $a$  and  $b$ . To get the average distance one averages  $r_{ab}$  over all pairs of nodes on the tree and over all trees in the

ensemble. The result is that for homogeneous trees the average distance behaves for large  $N$  as [20, 21, 24]:

$$\text{hri}_h \stackrel{p}{\sim} \frac{1}{N}; \quad (11)$$

while for causal ones<sup>2</sup> [25, 31]:

$$\text{hri}_c \sim \ln N: \quad (12)$$

The power-law growth of the linear extent  $\text{hri}_h \sim N^{1/2}$  with the system size means that homogeneous trees have fractal dimension  $d_h = 2$ , while the behavior  $\text{hri}_c \sim \ln N$  that the fractal dimension of causal trees is  $d_c = \infty$ . The separation of vertices on a causal tree is very small and the whole tree structure is compactly concentrated around the oldest part of the tree.

This can be well illustrated by studying the two-point correlation function  $G_N^{(2)}(r)$ :

$$G_N^{(2)}(r) = \frac{1}{N^2} \sum_{ab}^* \delta(r - r_{ab}) : \quad (13)$$

The delta function  $\delta(r - r_{ab})$  selects only pairs  $a;b$  separated by  $r$  edges. The two-point function can be thus interpreted as the probability that two randomly chosen nodes of the tree are separated by  $r$  links. Alternatively it can be interpreted as the distance distribution giving the fraction of nodes at a distance  $r$  from a randomly chosen one. By construction,  $\sum_r G_N^{(2)}(r) = 1$  and  $G_N^{(2)}(0) = 1/N$ . The average distance between vertices is given by the mean value of the two-point function:

$$\text{hri} = \sum_{r=1}^{\infty} r G_N^{(2)}(r): \quad (14)$$

The two-point function gives a very valuable information about the distance distribution in the given ensemble of graphs. In figure 4 we compare the two-point function  $G_{hN}^{(2)}(r)$  for homogeneous and  $G_{cN}^{(2)}(r)$  for causal trees of the same size  $N = 1000$ . One sees that indeed the typical causal trees are much shorter than homogeneous. The distance distribution for causal trees is much more concentrated.

One can analytically derive the shape of the two-point function  $G_{hN}^{(2)}(r)$  for homogeneous trees in the limit of  $N \rightarrow \infty$ . In this limit one can approximate the shape by a function of a continuous variable:

$$G_{hN}^{(2)}(r) \sim \frac{ar}{N} \exp\left(-\frac{ar^2}{2N}\right); \quad (15)$$

where  $a$  is a positive constant. We have:

$$\int_0^{\infty} dr G_{hN}^{(2)}(r) = 1; \quad (16)$$

---

<sup>2</sup> In the references [25, 31] only the distribution of distances from the root was calculated.

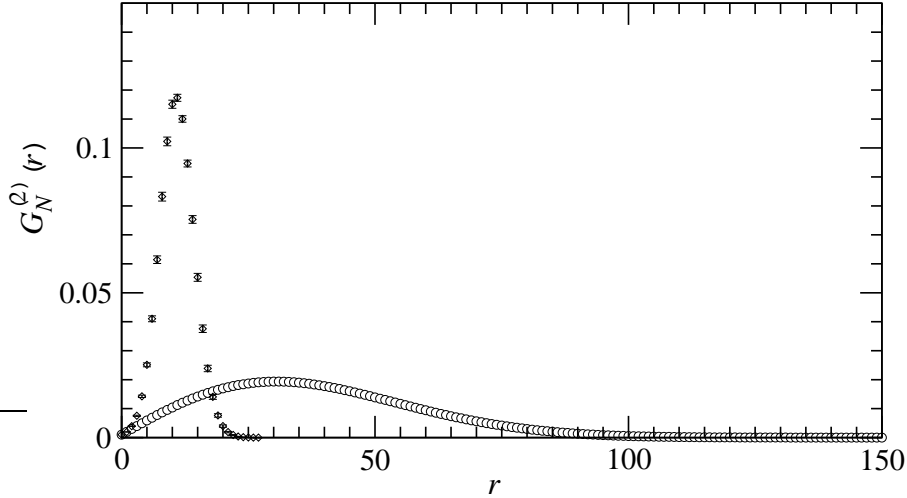


**FIGURE 4.** The distance distribution functions for the homogeneous (circles) and causal trees (diamonds) for  $N = 1000$ . Error bars for data points represented by circles are smaller than the symbol size.

and

$$\lim_{N \rightarrow \infty} \frac{1}{N} \int_0^{\infty} dr r G_{hN}^{(2)}(r) = \frac{p}{a} : \quad (17)$$

In the large  $N$  limit the two-point function becomes effectively an  $N$ -independent function of the scaling variable  $x = r = \frac{N}{a}$ :

$$G_{hN}^{(2)}(r) dr = g_h(x) dx = x e^{-x^2/2} dx : \quad (18)$$

When one draws the two-point functions for different system sizes as a function of the scaling variable the corresponding curves collapse to a universal shape independent of  $N$ . It will be illustrated below for the scale-free graphs.

Similarly, we expect that the two point-function for causal trees scales in the variable  $x = r = \ln N$ :

$$G_{cN}^{(2)}(r) dr ! \quad g_c(x) dx ; \quad (19)$$

which implies (12). Such scaling indeed holds. The shape of the scaling function can be well approximated by a Gaussian function:

$$g_c(x) = e^{bx} e^{-x^2/2} ; \quad (20)$$

where  $b$  is a constant. The two systems have thus completely different scaling and distance distribution profiles.

Also the other statistical characteristics of the causal trees are different from those for the homogeneous trees. For instance one can determine the node degree distribution averaged over trees in the ensemble:

$$p(q) = \frac{1}{N} \sum_a \delta(q - q_a) : \quad (21)$$

Here  $q_a$  is the degree of node  $a$ , the sum runs over all nodes of the tree, and the average is over all trees in the ensemble. If one calculates this distribution for the homogeneous trees one obtains:

$$p_h(q) = \frac{e^1}{(q-1)!}; \quad (22)$$

while for causal trees:

$$p_c(q) = 2^q : \quad (23)$$

Again we see the difference between the set of all labeled trees and the subset of causally labeled trees.

So far we have discussed the ensembles of unweighted graphs: each labeled graph has had a statistical weight equal to  $1=N!$  independently of its shape. One can easily extend those considerations to the ensembles of weighted graphs, in particular to an ensemble of graphs for which the statistical weight includes a factor depending on node degrees (2). For instance, one can analytically solve a model of trees (both causal and homogeneous) whose statistical weight is a product of weights depending on individual node degrees. For each node one introduces a weight which is a function of the number of edges emerging from it. By tuning the weights one can obtain trees with a desired degree distribution. However, the following question arises: assume that we have two ensembles of trees with the same node degree distribution. In the first ensemble we have all labeled trees and in the second only causally labeled ones. We now remove labels from the trees. All we have is the graph topology. Can we distinguish whether a given graph topology comes from homogeneous or causal graph ensemble? One can answer this question in the affirmative.

Let us sketch the solution. We will generate scale-free tree graphs by tuning the nodes weights. Introducing this to the model, one has to modify the right-hand side of the self-consistency equations. The exponential series which we used before in equations (5) and (8) to generate equally weighted trees has to be substituted by:

$$\sum_{k=0}^{\infty} \frac{Z^k}{k!} : \sum_{k=0}^{\infty} \frac{w(k+1)Z^k}{k!} : \quad (24)$$

Here  $w(q)$  is the node weight which depend only on node's degree  $q$ . It can be also interpreted as branching ratio that a link will split into  $q-1$  links. In the previous case the weights  $w(q) = 1$  were identical for all  $q$ 's. In order to produce scale-free networks with the Barabási-Albert distribution:

$$p_{BA}(q) = \frac{4}{q(q+1)(q+2)}; \quad (25)$$

one has to choose  $w_c(q) = (q-1)!$  for causal trees and  $w_h(q) = (q-1)!p_{BA}(q)$  for homogeneous trees. In the limit of  $N! \rightarrow \infty$  these two ensembles have identical node-degree distributions  $p_c(q) = p_h(q) = p_{AB}(q)$ . To illustrate this we show in figure 5 node degree distributions obtained by Monte-Carlo simulations of causal and homogeneous trees with the appropriately chosen branching weights. One can see that they perfectly follow the distribution (25). In other words, one cannot distinguish to which ensemble

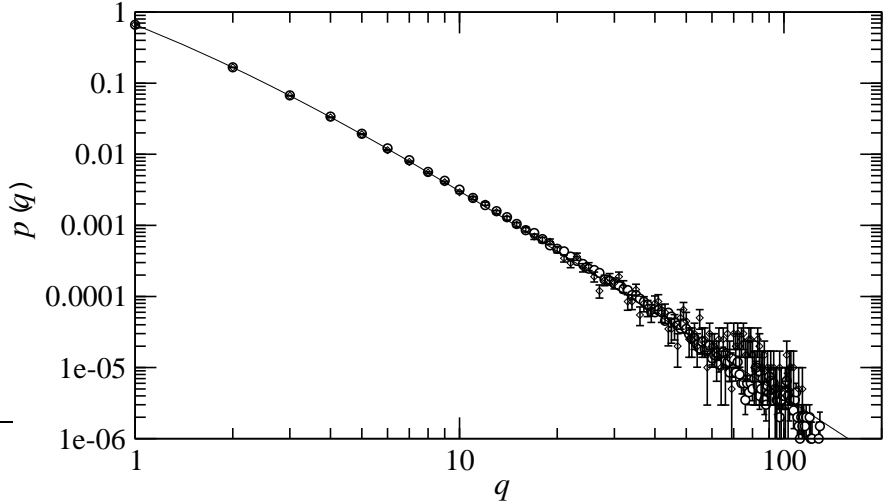


**FIGURE 5.** The degree distribution for causal (diamonds) and homogeneous (circles) scale-free trees measured in Monte-Carlo runs for  $N = 1000$ . One sees that they are statistically identical.

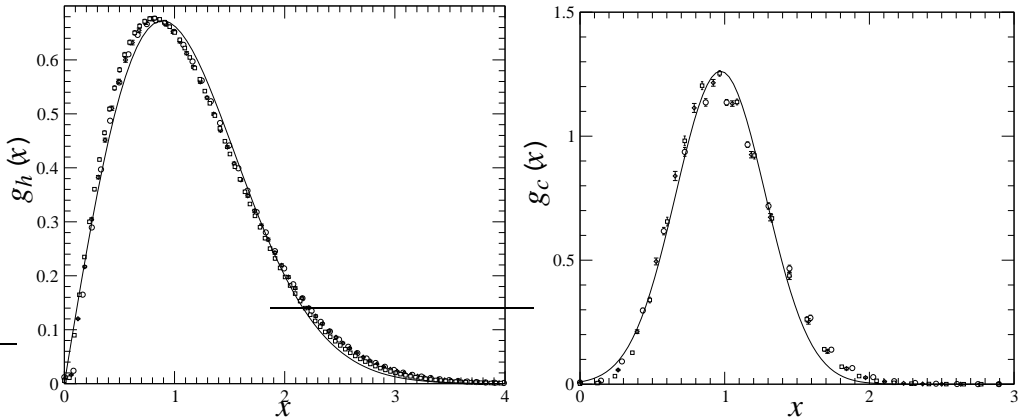


**FIGURE 6.** Left: The distance distributions for homogeneous trees plotted in the rescaled variable  $x = r - \frac{1}{N} \ln N$  for different  $N$ :  $N = 500, 1000, 2000, 4000$ . The continuous line is given by the function  $b x \exp(-ax^2/2)$  (18). Right: The distance distributions for causal trees plotted in the rescaled variable  $x = r - \ln N$  for different  $N$ :  $N = 500, 1000, 2000, 4000$ . The continuous line is given by a Gaussian fit (20). The small deviations from this curve may be attributed to the finite size effects. The deviations are much less for unweighted graphs.

the tree belongs just by measuring nodes degrees. One can however distinguish the ensembles very easily if one determines the distance distribution  $G_N^{(2)}(r)$ . As before, the causal trees have an infinite fractal dimension, while the homogeneous ones the fractal dimension equal to two. The distance distribution  $G_N^{(2)}(r)$  for homogeneous trees is plotted in the scaling variable  $x = r - \frac{1}{N} \ln N$  on the left-hand side of figure 6 and for causal trees in the scaling variable  $x = r - \ln N$  on the right-hand side. As expected in both cases the data collapses to a curve independent of  $N$ . The average distance scales as  $\langle r \rangle_h \sim \frac{1}{N} \ln N$  in the first case while as  $\langle r \rangle_c \sim \ln N$  in the second. Note that we have

introduced a logarithmic correction to the square root scaling (11) and (18) for the scale-free homogeneous trees. This is due to the fact that in this case the series (24) develops a logarithmic singularity. This correction does not affect the fractal dimension which is still two. The average distance scales as

$$\text{hr}_h \stackrel{P}{\sim} \frac{1}{\ln N} : \quad (26)$$

The distribution (25) belongs to a broader class of scale-free distributions [31]:

$$p_{KR}(q) = \frac{(2 + \omega)\Gamma(3 + 2\omega)}{\Gamma(1 + \omega)} \frac{\Gamma(k + \omega)}{\Gamma(k + 3 + 2\omega)}; \quad (27)$$

which emerge as the limiting distributions in a growth process with the linear attachment kernel  $A_q = q + \omega$ ,  $\omega > 1$ . The BA distribution (25) corresponds to  $\omega = 0$ . The mean value of the  $p_{KR}(q)$  distribution is equal two:  $\sum_q q p_{KR}(q) = 2$  for all  $\omega > 1$ , in accordance with the average number of links per node on a tree. For large  $q$  the distributions have a power-law tail:  $p_{KR}(q) \sim q^{-\gamma}$  with the exponent  $\gamma = 3 + \omega$ , which assumes the value from the range  $\gamma > 2$ . Interestingly enough, for the scale-free causal trees (27) the average distance scales logarithmically  $\text{hr}_c \sim \ln N$  independently of  $\gamma$ , whereas the scaling properties of the homogeneous trees strongly depend on  $\gamma$ . In particular the average distance scales as  $\text{hr}_c \sim N^{1-d_f}$  where [22, 23, 24]

$$d_f = \max \left( 2; \frac{\gamma - 1}{\gamma} \right) : \quad (28)$$

We have  $d_f = 2$  for  $\gamma > 3$ . For  $2 < \gamma < 3$  the fractal dimension  $d_f$  assumes values which continuously grow from two to infinity while  $\gamma$  decreases from three to two. Please note that the logarithmic corrections appear for  $\gamma = 3$ . Those corrections can be interpreted as the fact that at this point  $\text{hr}_c$  grows slower than  $\frac{1}{N}$  but faster than any power  $N^{1-2-\varepsilon}$  with  $\varepsilon > 0$ .

The discussion of this section can be summarized as follows. We have considered four ensembles of trees: (a) homogeneous uniformly weighted, (b) causal uniformly weighted, (c) homogeneous with the BA scale-free distribution (25), (d) causal weighted with the BA scale-free distribution. The average distance between nodes in a scale-free system is generally smaller than in a random one: so graphs in the ensemble (c) have on average smaller diameter than in (a) and in (b) than in (d). This effect is well known. It is related to the presence of nodes with high degree which cluster around themselves many vertices just in distance one. Another effect which is less known is that the causality lowers the distances between nodes on the graph. The effect caused by causality is even stronger than by scale-free tails: the graphs in (b) have diameter much smaller than those in (a), and similarly those in (c) than those in (d). One observes big changes if one imposes the causality constraint. The reason why causality plays such an important role in enhancing the small world effect is related to the fact that the oldest vertices, in addition to having highest degrees, cluster with each other forming a kernel of the graph with extremely high connectivity. Remaining nodes tidily surround this compact kernel making the whole graph structure jampacked. In figure 7 we compare the distance

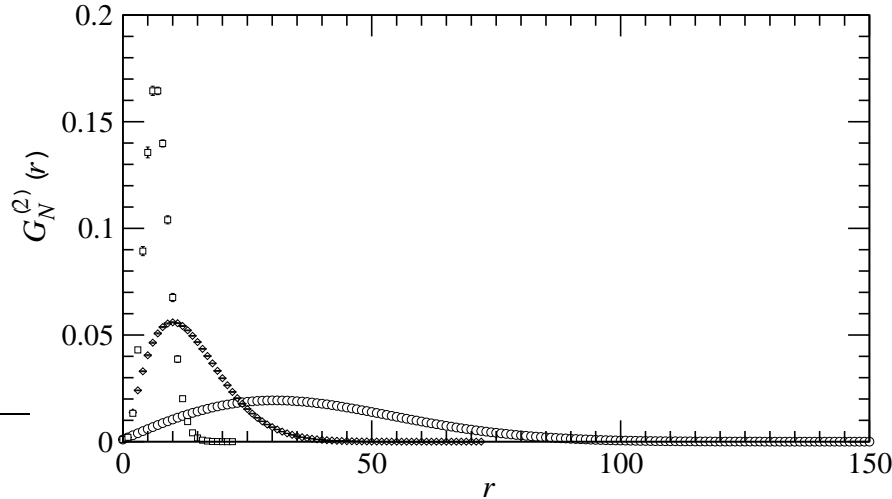


**FIGURE 7.** The distance distribution  $G_N^{(2)}(r)$  for  $N = 1000$  for unweighted homogeneous tree (circles), scale-free homogeneous trees (diamonds) and scale-free causal trees (squares).

distribution  $G_N^{(2)}(r)$  for the cases (a), (c) and (d) for the same system size. We see that homogeneous graphs (a) are more elongated than causal ones (c) which in turn are more elongated than causal scale-free ones (d). We have not shown the case (b) in the figure in order to keep it transparent. The case (b) was compared to (a) in the figure 4.

## CONDENSATION

Statistical ensemble of causal trees discussed in the previous section is for the weights  $w(q) = \Gamma(q + \omega) = \Gamma(1 + \omega)$  [25] equivalent to an ensemble of trees obtained by a growth process with the linear attachment kernel  $A_q = q + \omega$  [31]. The map between these models is mathematically exact. For non-linear kernels the two models slightly differ but both display the same features<sup>3</sup>. If one applies a superlinear attachment kernel in the growth process:  $A_q = q^\sigma$  for  $\sigma > 1$  one sees the appearance of a singular node which has the degree proportional to the size of the tree. If one applies a sublinear kernel  $\sigma < 1$ , the degree distribution will be suppressed exponentially for large  $q$ . The linear kernel is marginal in the sense that it lies exactly between the phase with the singular node and the exponential tail. A very similar situation takes place for homogeneous trees but the mechanism of the emergence of the singular node is different. The model can be mapped onto a balls-in-boxes model [30]. In order to obtain scale-free trees one has to choose appropriate vertex weights of the model. Any deviation from the fine-tuned values results in either the appearance of the singular node or the exponential suppression in the node degree distribution, exactly as for growing networks. Roughly speaking, if we denote the fine-tuned scale-free distribution  $p_0(q) = q^{-\gamma}$  (the second case in the equation below)

---

<sup>3</sup> see however the reference [27].

we have three possible scenarios:

$$\begin{aligned}
 p(q) & \stackrel{8}{<} p_0(q) e^{-\mu q} ; \\
 & \stackrel{1}{=} p_0(q) ; \\
 & \stackrel{2}{:} p_0(q) + \frac{1}{N} \delta(q - \rho N) ;
 \end{aligned} \tag{29}$$

In the first case the typical fluctuations of the node degree are of order  $1=\mu$  independently of  $N$ . In the third case there is a singular node with an extensive number of links  $q = \rho N$ . This is equivalent to the backgammon condensation of the balls-in-boxes model [30]. The appearance of the singular node makes the system to be even more compact than for scale-free graphs. The distance between nodes increases slower than logarithmically since many vertices are in the closest neighborhood of the singular node. In the extreme case which corresponds to the star topology – a vertex surrounded by  $N - 1$  vertices – the average distance is smaller than two and is independent of  $N$ .

Is the condensation a feature of the tree graph ensemble, or it is observed for ensembles of graphs as well? We have studied this question for homogeneous scale-free graphs and pseudographs. In our conventions graphs do not have multiple- and self-connecting edges while pseudographs do. For graphs, the condition that they have neither multiple- nor self-connections acts as strong constraints on the graph structure which are sometimes called structural constraints [28, 29]. In particular they strongly prevent the system from developing a power-law tail in the node-degree distribution for finite size systems [28, 29]. It also turns out they prohibit the condensation which we discussed above. So far we have not found any evidence for the backgammon condensation for graphs and the emergence of singular node on the graph. On the contrary, for pseudographs the situation is very much like for trees and one observes the condensation. We simulated a canonical ensemble of homogeneous pseudographs with  $L$  links and  $N$  vertices, with the distribution  $p_{BA}(q)$  (25). This was achieved by tuning the node degree weights, similarly as we have described for trees before, and by adjusting the ratio  $\bar{q} = 2L=N$  by choosing  $L = N$  to the mean value of the distribution  $\bar{q}_i = \sum_q q p_{BA}(q) = 2$ . Indeed the system produced the desired distribution. The next step was to check how the system reacts on the change of the number of links. We had increased the number of links  $L$  while keeping the number of nodes  $N$  constant so that the ratio  $\bar{q} = 2L=N = 4$  exceeded  $\bar{q}_i = 2$ . The system reacted as follows. The distribution of the bulk part was as before equal to the desired power-law distribution  $p_{BA}(q)$  but the system additionally produced a singular node which took the surplus of links. The presence of the singular node is manifested as a peak in the distribution. The position of the peak moves linearly with the system size and the peak departs from the main body of the distribution. Its height is proportional to  $1=N$  since it is a probability of picking up one out of  $N$  vertices. The situation is depicted in figure 8. This is an example of the backgammon condensation [30]. If one adds more links, then the surplus will go to the singular node. One can see this effect by comparison of the plots in the left- and right-hand side of figure 8 which differ by the ratio  $\bar{q} = 2L=N$  and the positions of the peak correspondingly. If one chooses the ratio  $\bar{q} = 2L=N$  to be smaller than  $\bar{q}_i$  the system generates an exponential tail in the node degree distribution. This is again what one expects from the balls-in-boxes model. The reason why this analogy works for pseudographs and does not for graphs is that for pseudographs the degrees of individual vertices are almost independent of each other

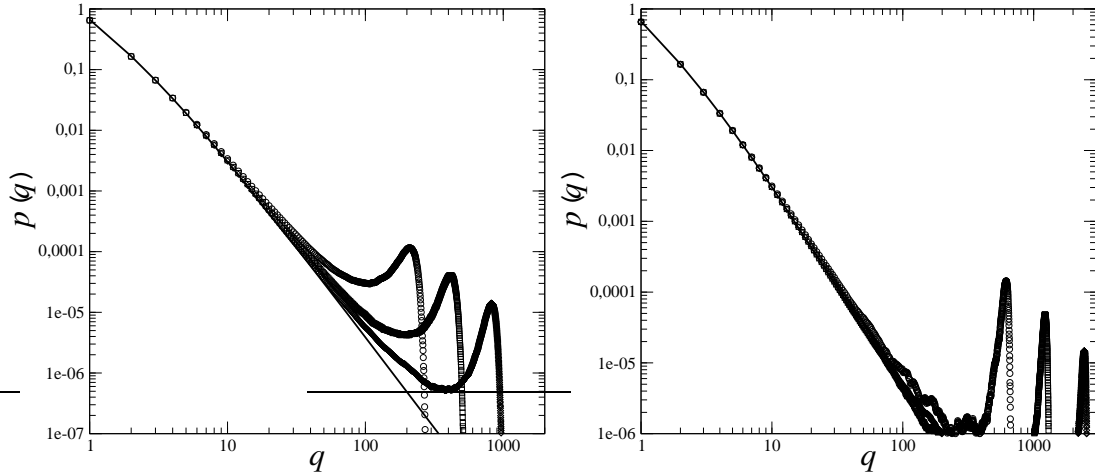


**FIGURE 8.** Left: The node degree distribution for scale-free pseudographs with  $\bar{q} = 2L = N = 4$  which is above the condensation threshold  $hq_1 = 2$  of the BA distribution (25). The main part of the distribution goes along the limiting BA curve (solid line). The peak represents the singular vertex. Its position moves linearly with the system size  $N = 200; 400; 800$ . Right: The same for larger link density:  $\bar{q} = 2L = N = 8$ .

except of the global constraint  $q_1 + q_2 + \dots + q_N = 2L$ , while they are in a subtle way correlated for graphs due to the structural constraints.

## SUMMARY

We have applied methods of statistical mechanics to compare ensembles of homogeneous and causal (growing) networks. We have shown that the causality strengthens the small world effect due to clustering of nodes with high connectivity in the kernel of the graph. In particular, for homogeneous random trees the average inter-node distance scales as  $\sqrt{N}$  while for causal networks as  $\ln N$ . We have compared two ensembles of random trees with Barabási-Albert distribution and observed that despite they have identical degree distribution, the causal trees have much smaller diameter than the corresponding homogeneous trees.

We have also discussed the stability of the scale-free distributions. For growing network such distributions emerge for linear attachments kernels. If the attachment is slightly perturbed the system either exponentially suppresses nodes with higher degree or develops a singular node with a degree proportional to the total number of links. The first type of perturbation corresponds to sublinear while the second to superlinear kernels. Similar instabilities are observed for homogeneous pseudographs. Scale-free distributions require a fine-tuning of the weight parameters. A slight perturbation, as before, also leads either to the exponential suppression or to the emergence of a singular node on the graph. In this case the singular node emerges as a result of a condensation of the backgammon type [30].

## ACKNOWLEDGMENTS

This is essentially a review paper. Most of the results presented above were obtained by the Krakow-Orsay collaboration, including Jerzy Jurkiewicz and André Krzywicki. We wish to thank Jerzy and André for their contribution. ZB thanks the organizers of the conference CNET2004 for the invitation. This work was partially supported by the Polish State Committee for Scientific Research (KBN) grant 2P03B-08225 (2003-2006) and by EU IST Center of Excellence “COPIRA”.

## REFERENCES

1. R. Albert and A-L Barabási, *Rev. Mod. Phys.* **74**, 47 (2002).
2. S. N. Dorogovtsev and J. F. F. Mendes, *Adv. Phys.* **51**, 1079 (2002).
3. M. E. J. Newman, *SIAM Review* **45**, 167 (2003).
4. R. Albert and A-L Barabási, *Science* **286**, 509 (1999).
5. H.A. Simon, *Biometrika* **42**, 425 (1955).
6. Z. Burda, J. D. Correia and A. Krzywicki, *Phys. Rev. E* **64**, 046118 (2001).
7. A. Krzywicki, cond-mat/0110574.
8. J. Berg and M. Lässig, *Phys. Rev. Lett.* **89**, 228701 (2002).
9. S. N. Dorogovtsev, J. F. F. Mendes and A. N. Samukhin, *Nucl. Phys. B* **666**, 396 (2003).
10. Z. Burda, J. Jurkiewicz and A. Krzywicki, *Phys. Rev. E* **69**, 026106 (2004).
11. I. Farkas, I. Derenyi, G. Palla and T. Vicsek, *Springer Lect. Notes Phys.* **650**, 163 (2004).
12. J. Park and M. E J. Newman, *Phys. Rev. E* **70**, 066117 (2004).
13. D.-S. Lee, K.-I. Goh, B. Kahng, and D. Kim, *Nucl. Phys. B* **696**, 351 (2004).
14. L. Bogacz, Z. Burda and B. Waclaw, cond-mat/0502124.
15. P. Erdős and A. Rényi, *Publ. Math. Debrecen* **6**, 290 (1959).
16. P. Erdős and A. Rényi, *Publ. Math. Inst. Hung. Acad. Sci.* **5**, 17 (1960).
17. B. Bollobás, *Random Graphs* Academic Press, New York (1985).
18. G. Polya, R.C. Read, *Combinatorial Enumeration of Groups, Graphs, and Chemical Compounds*, Springer, New York (1987).
19. J. Ambjørn, B. Durhuus, J. Fröhlich, P. Orland, *Nucl. Phys. B* **270**, 457 (1986).
20. J. Ambjørn, B. Durhuus, T. Jonsson, *Phys. Lett. B* **244**, 403 (1990).
21. P. Bialas, *Phys. Lett. B* **373**, 289 (1996).
22. P. Bialas, Z. Burda, *Phys. Lett. B* **384**, 75 (1996).
23. J. Jurkiewicz, A. Krzywicki, *Phys. Lett. B* **392**, 291 (1997).
24. P. Bialas, Z. Burda J. Jurkiewicz, *Phys. Lett. B* **421**, 86 (1998).
25. P. Bialas, Z. Burda, J. Jurkiewicz, A. Krzywicki, *Phys. Rev. E* **67**, 66106 (2003).
26. Z. Burda, J. Erdmann, B. Petersson, M. Wattenberg, *Phys. Rev. E* **67**, 026105 (2003).
27. P. Bialas, *Acta Phys. Pol. B* **34**, 4699 (2003).
28. Z. Burda and A. Krzywicki, *Phys. Rev. E* **67**, 046118 (2003).
29. M. Boguñá, R. Pastor-Satorras and A. Vespignani, *Eur. Phys. J. B* **38**, 205 (2004).
30. P. Bialas, Z. Burda and D. Johnston, *Nucl. Phys. B* **493**, 505 (1997).
31. P.L. Krapivsky, S. Redner, *Phys. Rev. E* **63**, 66123 (2001).
32. F. Harary, E.M. Palmer, *Graphical Enumeration*, Academic Press (1973).